Deep Reinforcement Learning based Interference Optimization for Coordinated Beamforming in Ultra-Dense Wi-Fi Networks

Jamshid Bacha[a], Anatolij Zubow[a], Szymon Szott[b], Katarzyna Kosek-Szott[b], Falko Dressler[a,*]

[a]*School of Electrical Engineering and Computer Science, TU Berlin, Germany*
[b]*AGH University of Kraków, Poland*

Abstract

Next-generation Wi-Fi networks are expected to have an ultra-dense deployment of access points (APs), thus, interference from overlapping basic service sets (OBSSs) poses challenges for interference management. Wi-Fi 8 aims at mitigating such interference using multi-access point coordination (MAPC). One of the MAPC variants is coordinated beamforming (Co-BF), where neighboring APs direct their signals towards specific users. Besides beam steering, APs can also perform null steering, which is more complex but can bring greater performance gains. In this paper, we present a centralized approach named intelligent null steering by reinforcement learning (IntelliNull), designed to reduce interference from neighboring transmitters by coordinated nulling while maximizing the signal quality at each station. We show that training the beam and null steering mechanism with a deep deterministic policy gradient (DDPG), it is possible to steer beams toward associated stations while intelligently nulling the most destructive interference from OBSS rather than nulling random interference directions. This method enhances communication between the AP and neighboring stations by reducing channel access contention, enabling transmissions at full power, and reducing worst-case latency. The proposed IntelliNull agent continuously adapts to changes in the network environment, including node mobility using channel state information (CSI) collected in real-time. We also compare our IntelliNull, which is based on beamforming plus nulling, with the baseline which is based on beamforming only. Our results demonstrate that IntelliNull outperforms the baseline by effectively mitigating interference, leading to higher throughput and better signal-to-interference-plus-noise ratio (SINR), especially in dense deployment scenarios where beamforming alone fails to sufficiently suppress OBSS interference.

Keywords: Wi-Fi 8, Overlapping basic service set, Multi-access point coordination, Interference management, Coordinated beamforming, Reinforcement learning, Deep deterministic policy gradient

1. Introduction

The use of Wi-Fi has increased significantly in recent years due to the rapid development of user devices such as smartphones, smart glasses, and, recently, virtual reality (VR) sets [1]. This proliferation of Wi-Fi devices and the increasing demand for bandwidth is the source of increased inter-network interference [2, 3]. While the use of technologies such as large-scale multiple input multiple output (MIMO) antenna systems can significantly enhance network capacity by leveraging spatial multiplexing [4], there remains the problem of interference among networks of neighboring access points (APs), called overlapping basic service sets (OBSSs) [5]. Such OBSSs create a major challenge, limiting Wi-Fi's ability to deliver consistent performance in ultra-dense deployments because of decreasing signal-to-interference-plus-noise ratio (SINR), disorganized infrastructure, and limited spectrum resources [6, 7]. One possible solution to this problem, enabled by the development of MIMO antenna systems, is an advanced beamforming technique called coordinated beamforming (Co-BF) [8, 9]. Co-BF is enabled by multi-access point coordination (MAPC), which involves multiple APs working together to direct their signals to specific users. This technique improves signal quality and reduces interference, leading to better overall network performance. By coordinating their actions, APs can avoid conflicts and optimize the network for better performance. This coordinated beamforming feature is part of the upcoming IEEE 802.11bn (Wi-Fi 8) standard and will allow APs in an OBSS setting to coordinate their transmissions not only by steering beams towards receivers but also suppressing interference by placing radiation nulls towards neighboring (non-associated) stations [10]. Therefore, this advancement enables simultaneous transmissions across multiple OBSSs on the same channel, significantly improving spectral efficiency [11].

Figure 1 illustrates how beamforming and nulling techniques can mitigate interference in neighboring Wi-Fi networks. In the presented example, station 1 is associated

*Corresponding author
Email addresses: bacha@ccs-labs.org (Jamshid Bacha), zubow@ccs-labs.org (Anatolij Zubow), szymon.szott@agh.edu.pl (Szymon Szott), katarzyna.kosek-szott@agh.edu.pl (Katarzyna Kosek-Szott), dressler@ccs-labs.org (Falko Dressler)

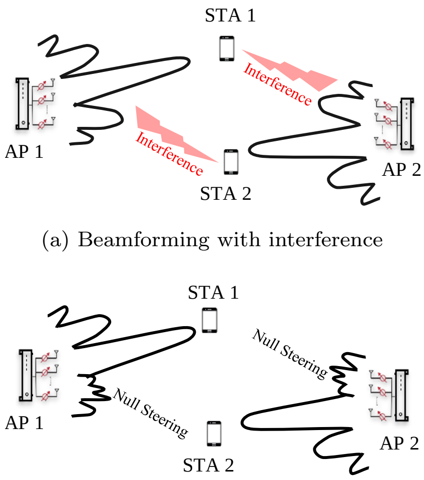

(a) Beamforming with interference

(b) Beamforming with null steering

Figure 1: Conceptual example of Co-BF: APs transmit simultaneously using (a) beamforming (to improve signal strength at receiver) and (b) null steering (to reduce interference).

with AP 1, and station 2 is associated with AP 2. First, both APs use beamforming to direct their signal to their associated stations, to improve communication efficiency (Figure 1a). However, in addition to the main lobe, there are also side lobes that can cause interference to receivers in neighboring networks (e.g., station 2 receives interference from AP 1). Therefore, since the APs operate in a coordinated mode and know the intended receivers of neighboring transmissions and their placement, these APs additionally use null steering to minimize the signal strength in the direction of the stations communicating with the other APs (Figure 1b). As a result, both APs can communicate with their respective stations simultaneously without causing mutual interference, leading to improved throughput and reduced latency [12]. Co-BF is therefore a promising solution to mitigate interference caused by OBSSs.

Even though Co-BF and null steering provide a promising solution to mitigate interference in ultra-dense multi-AP Wi-Fi 8 networks, several challenges remain unaddressed. For example, consider the scenario depicted in Figure 1 and assume each AP is equipped with four antennas and serves a large number of stations. In such a setup, AP 1 would ideally need to null the interference towards stations associated with neighboring AP 2. However, with only four antennas, AP 1 has a maximum of four spatial degrees of freedom (DoF) available. Since one DoF is required for beamforming toward its own associated station, only three DoFs remain to create nulls. Thus, AP 1 can effectively null out interference in at most three directions, suppressing its signals toward the most critical non-associated stations that are affected the most by its transmissions. In addition, installing a large number of antennas like in massive MIMO [13] is not a feasible solution based on the cost and size of the APs. If the AP randomly selects which directions to null, it risks reducing the gain of the main lobe toward its own associated station, thus degrading overall performance. Therefore, intelligently identifying and nulling only the most critical interfering directions becomes crucial. So, the present study uses centralized coordination among APs (e.g., via MAPC), where each AP is aware of the scheduling information and the channel state information (CSI) of stations in its neighborhood. This assumption is consistent with the Wi-Fi 8 architecture. Our model considers information from all stations to predict appropriate null directions, effectively addressing the listed challenges.

A further challenge in coordinated null steering is the establishment of a coordination set: APs must know which stations are scheduled during the transmission opportunity (TXOP) to suppress interference effectively. Identifying an optimal nulling configuration is complex, as the number of possible configurations grows exponentially with the number of APs M, the number of antennas per AP N_t, and the number of users N_u in the OBSS. Specifically, the total number of configurations is represented by $\binom{N_u}{N_t}^M$, which can create a vast search space. This combinatorial explosion makes exhaustive search computationally infeasible. Moreover, stations in the network may move continuously, changing their positions even every few milliseconds. This transforms the problem into a one-shot decision-making scenario, where the system must select nulling directions within fractions of a second. Hence, a scalable solution must rely on intelligent selection strategies to efficiently identify high-impact nulling directions without exhaustive enumeration. Instead of exhaustively searching through all possible nulling configurations, our reinforcement learning (RL)-based approach learns a nearly optimal nulling strategy.

Another important challenge is the availability of correct CSI, not only locally but also at stations in the OBSS. Wang et al. [14] indicate that the mobility of the stations introduces rapid variations in the channel conditions. Therefore, frequent updates are essential to keep accurate CSI. As the overhead caused by channel sounding becomes significant, the performance of the network degrades. Despite the outdated CSI caused by mobility, the intelligent null steering by reinforcement learning (IntelliNull) system maintains high performance, highlighting its robustness against dynamic wireless environments. Unlike conventional methods that attempt to null random interfering directions, IntelliNull learns to null only the most destructive interference sources. This selective nulling strategy preserves spatial DoF for beamforming, ensuring that the main lobe remains as strong as possible for intended stations, thereby improving the overall throughput.

The design of Co-BF shares some similarities with coordinated multi-point (CoMP) [15]. Both techniques aim to enhance spatial reuse and improve user throughput in dense wireless networks through coordinated transmission strategies, exchange of CSI between APs, and mitigating interference by steering signal energy toward intended users while shaping the spatial radiation pattern to reduce interference elsewhere [16, 17]. However, there are also notable differences. CoMP allows for the cancellation of interference signals from neighboring cells by coordinating the transmission and reception of signals from different base stations (BSs), our approach focuses specifically on Wi-Fi where each AP serves its own associated station while intelligently placing radiation nulls toward major interference stations in neighboring OBSSs.

All the limitations mentioned above motivate the search for adaptive beamforming and interference control methods that leverage machine learning (ML) tools to adapt the learned interference direction based on the environment and hardware surveyed in [18, 19]. Unlike traditional methods that focus solely on beamforming optimization, this work emphasizes RL-based nulling design to effectively suppress interference in multi-AP Wi-Fi 8 (IEEE 802.11bn) environments. The focus is to achieve network performance in a scenario having densely deployed APs and many stations associated with each AP, i.e., a typical OBSSs scenario.

This paper addresses the research gap described by introducing our IntelliNull approach for null configuration and coordination between APs. IntelliNull intelligently steers nulls toward non-associated stations to mitigate interference caused by the AP's own transmissions. By integrating null steering with beamforming, IntelliNull outperforms conventional beamforming-based approaches, achieving superior SINR and throughput, particularly in dense Wi-Fi deployments. It outperforms the classical uncoordinated beamforming methods and enables RL-based space division multiplexing in OBSS. The proposed RL approach offers competitive performance compared to an oracle-based model as a benchmark, which uses exhaustive search to find the best beamforming and interference nulling configuration. We conduct a large-scale set of simulation experiments studying the performance of null steering in Co-BF to evaluate its impact on interference suppression and the resulting throughput in the overall network.

Our main contributions can be summarized as follows:

- IntelliNull is a centralized RL framework that optimizes interference mitigation through intelligent null steering.
- This study demonstrates that the performance of this system based on imperfect CSI approaches a theoretical oracle, which perfectly optimizes the beams and nulls of all APs under perfect CSI.
- We provide a systematic comparison between Co-BF based on beamforming only versus beamforming combined with null steering, showing that coordinated beamforming with selective nulling significantly improves system performance.
- Results show that intelligent suppressing interference toward the most affected non-associated stations can improve throughput and SINR compared to random nulling.
- Despite increased interference dynamics caused by station mobility, the IntelliNull agent consistently identifies near-optimal nulling strategies under realistic mobility scenarios.
- We show that by reducing interference through targeted null steering, our system significantly reduces channel access contention in dense deployments, enabling higher medium utilization, lower latency, and improved throughput.
- The RL agent achieves fast convergence, enabling effective adaptation even in dynamic networks with mobile stations.

The remainder of the paper is organized as follows. We study related work on interference modeling and mitigation, ML-based optimization in wireless networks, and Co-BF in Section 2. We explain the system model for multi-AP coordination in Section 3. We introduce our novel IntelliNull platform in Section 4. In Section 5, we present results from a thorough performance evaluation. Finally, we conclude the paper in Section 6.

2. Related Work

We first review the literature in the area of interference modeling and mitigation in Wi-Fi networks. Then, we show how ML can support interference management. Next, we discuss research in the emerging topic of Co-BF and conclude with describing how our contribution fills the arising research gap.

2.1. Interference Modeling and Mitigation in Wi-Fi

Interference has always been a critical challenge in wireless communication, especially in dense Wi-Fi networks where devices operate in a shared spectrum. In recent years, various studies explored techniques for modeling and mitigating interference to improve network performance such as aligning interference to maximize DoF, reduce dependency on perfect CSI at the transmitters, and utilizing zero forcing and Maddah-Ali-Tse (MAT) scheme [20]. Borah et al. [21] propose a pre-coding technique with antenna and user selection to align interfering signals, enhancing network performance. They show that such methods can improve spectral efficiency in wireless networks.

Verma et al. [22] explore how OBSS contribute to interference issues and suggested Co-BF as a potential solution by leveraging multi-AP coordination where APs share CSI, interference levels, and transmission schedule to minimize interference between neighboring APs and improve overall network throughput. Along these, Nunez et al. [23] propose a MAPC framework for managing interference in dense AP Wi-Fi 8 environments, where APs share signal strength data with a central controller, which then forms spatial reuse-compatible AP groups and schedules their transmissions to reduce contention and optimize network performance.

Seyedebrahimi et al. [24] propose a software-defined network-based channel assignment algorithm for dense Wi-Fi networks, optimizing radio frequency (RF) channel assignment to reduce interference and improve spectral efficiency, evaluated through simulations showing significant performance improvements over existing methods. Abinader et al. [25] discuss the challenges Wi-Fi networks face in dense environments, particularly due to interference from overlapping networks. They propose a distributed interference coordination scheme to improve Wi-Fi performance in such scenarios and showed their scheme has significant improvements over existing methods like enhanced distributed channel access for downlink traffic.

Qiu et al. [26] examine the role of AP placement and channel selection in mitigating interference. Their research suggests that by carefully selecting the locations of APs and intelligently distributing them across different frequency channels, Wi-Fi networks can reduce OBSS and associated interference. The paper also highlights the impact of AP density on interference, showing that even small adjustments in AP placement can lead to notable improvements in stations throughput. Experimental results prove that four antennas AP serving one station can suppress up to 10 dB of interference towards neighboring stations [27]. Our focus is on the downlink channel, where 80–90 % of Wi-Fi traffic occurs [28]. These efforts underline the significance of interference modeling and the implementation of advanced mitigation techniques, such as Co-BF and power control for spatial reuse.

2.2. The Role of ML for Interference Management in Wireless Communication

The integration of ML, particularly deep learning (DL) and RL, into wireless communication systems represents a transformative shift in optimizing network performance and resource management. Most importantly, the recent success across DL in various fields has inspired its application in wireless communications. For example, Zhang et al. [34] employ four different supervised DL algorithms such as convolutional neural network (CNN), ResNet, convolutional long-short term deep neural network (CLDNN), and long short-term memory (LSTM) for interference source identification in Wi-Fi.

A study by Zhou et al. [35] focuses on using neural network (NN) for interference management and this showed a significant improvement in the network. Croce et al. [36] also use NN and hidden Markov chains for interference recognition in Wi-Fi with 95% accuracy. A DL based framework with generative adversarial network (GAN) is developed by Lin et al. [37] for interference mitigation in Wi-Fi technology. An advanced Q-learning based Wi-Fi AP is designed by Mishra et al. [38] where the system is very intelligent to find the interference-free channel and the system makes a decision intelligently based on mid and high interference levels by APs.

Interference can also be classified with DL models such as CNN approach used by Pulkkinen et al. [39], Schmidt et al. [40], and Kim et al. [41]. Robinson et al. [42] also use DL for the detection of interference and utilized CNNs to locate these signals with high accuracy for narrowband interference detection. Another study, by [43], first detects the interference signals and then classifies them into different categories such as continuous wave, Gaussian mixture, impulse interference, and narrowband interference using DL and multiple NN. DL achieve high classification accuracy between single-label and multi-label wireless signals for effective interference management and coexistence among different wireless technologies [44].

To overcome the difficulties of beamforming design, an ML-based approach to find the optimal beamforming vector is proposed by Kwon et al. [45]. Huang et al. [46] propose unsupervised DL-based algorithms with low complexity to achieve fast beamforming vectors. Zhang et al. [47] propose a novel multi-AP coordination system for Wi-Fi 7 networks using a centralized AP controller by utilizing deep Q-network (DQN) to enhance the channel access mechanism, aiming to maximize network throughput and maintain proportional fairness among multi-AP networks. A robust adversarial reinforcement learning (RARL) for coordinating multi-AP to handle interference from uncoordinated AP is discussed by Kihira et al. [48]. ML models are making great improvements in the field of wireless communication and also in the field of interference mitigation which highlights the importance of ML for interference management in Wi-Fi.

2.3. Coordinated Beamforming in Wi-Fi

Co-BF can reduce interference between APs that operate on the same channel, so it is expected to improve spatial reuse and overall network capacity. Pal et al. [49] confirm this observation by steering nulls towards non-associated stations to enable simultaneous data transmission in overlapping areas. Chauhan et al. [50] prove Co-BF enhances overall system performance, especially in dense network environments. Mohamed et al. [51] discuss the use of wireless gigabit (WiGig) APs operating in the 60 GHz frequency band to enable high-speed wireless local area networks (WLANs). The paper proposes a coordinated architecture for WiGig WLANs that integrates both the 5 GHz Wi-Fi and 60 GHz WiGig bands and finds that coordination manages simultaneous transmissions, reduce packet collisions, and minimize interference can improve the overall throughput. Mohamed et al. [52] demonstrate that coordinated beamforming enhances beam direction selection to maximize throughput while effectively mitigating interference, leading to improved network performance in Wi-Fi.

Zhang et al. [53] find that Co-BF significantly improves network performance in dense WLANs by selectively updating beamforming information for a subset of access points. Their research shows that Co-BF reduces beamforming overhead by 71% and enhances network throughput by 30.8%, demonstrating its effectiveness in maintaining up-to-date beamforming information and optimizing resource allocation. Coordination between multi-AP can improve

Reference	ML Model	Coordination	System Model	Critical Analysis
Afolabi et al. [29]	Q-learning	Coordinated/ Decentralized	Proposes an RL agent that optimizes transmission power levels to minimize interference and enhance network throughput	• Does not account for multi-AP Wi-Fi systems • Lacks coordinated beamforming and null steering in a specific direction • Does not consider co-channel interference and stations mobility in ultra-dense networks
Tarafder and Choi [30]	DQN	Coordinated/ Centralized	RL for coordinated interference management with beamforming vectors from a codebook	• No explicit null steering • Does not handle interference in ultra-dense OBSS • High training overhead due to predicting suboptimal beamforming vectors from a large codebook
Alkhateeb et al. [31]	NN	Coordinated/ Centralized	Uses NN for adaptive beamforming algorithms like Least Mean Squares and Linearly Constrained Minimum Variance to minimize interference	• Model may struggle to adapt to new or changing interference patterns since it is trained on a fixed dataset • Does not address null steering or interference management in an OBSS environment • Predicting beamforming vectors based on omni-received signals may be difficult in highly dynamic and dense environments
Wang et al. [32]	GPML	Coordinated/ Centralized	Uses a Max-SINR based beamforming compensation scheme to mitigate inter-BS interference, relying on GPML for channel estimation	• Uses GPML instead of RL for channel estimation • Method is less adaptive to dynamic interference since it depends on outdated CSI due to feedback delays • Uses a fixed infrastructure for small cells, making it difficult to adjust to changing conditions
Sun et al. [33]	DQN	Coordinated/ Distributed	Applies deep RL to predict coordinated beamforming strategies for managing interference in a wireless network	• Model does not account for the impact of moving stations • Focuses only on single-cell and does not address multi-AP coordination • Beamforming is delayed due to two sub-problems
Proposed Model	DDPG	Coordinated/ Centralized	RL-based IntelliNull platform for dynamic null steering in Wi-Fi	• Addresses multi-AP coordination • Optimizes null steering by prioritizing suppression toward the most severely impacted non-associated stations, preserving spatial DoF • Handles station mobility and operates robustly with imperfect CSI • Real-time nulling strategies instead of static codebooks or heuristic algorithms • Reduces channel access contention and improves throughput under dynamic network conditions

Table 1: The use of ML models in Co-BF for throughput improvement in wireless communication

spectral efficiency by sharing data and control information among APs, which enhances spectrum utilization, resulting in increased peak throughput, reduced latency, transmission reliability by reducing interference, and optimizing resource allocation, coordinated APs can attain precise phase and time synchronization which is crucial for avoiding mutual interference and maintaining high performance [54]. Moreover, centralized coordination facilitates efficient resource management, including resource scheduling, time synchronization, and data sharing among APs, leading to improved overall network performance. Dahrouj and Yu [55] explore the benefits of Co-BF in multi-cell multi-antenna wireless systems, unlike conventional systems that treat out-of-cell interference as noise, their approach allows multiple APs to jointly optimize their beamformers, improving overall system performance.

Azari and Masoudi [56] investigate interference management by comparing coordinated and uncoordinated access methods, highlighting that coordination can significantly improve system capacity and battery life. Their approach uses RL for distributed coordination. Analytical and simulation results show that for a packet loss requirement of 1%, the number of connected devices could be doubled by coordination. According to Chen et al. [57], each user's average delay changes with the number of small BSs increases in close proximity and with the increased number of small BSs, the transmission delay for each user increases because the interference from the small BSs to the users increases. Shakhatreh et al. [58] suggest different techniques for interference management with the increased number of BSs and recommended that coordination among BSs can reduce the interference in the overall system.

As wireless communication continues to evolve, the integration of coordinated strategies will play a vital role in maximizing spectrum efficiency and ensuring robust network performance. State-of-the-art research papers are summarized in Table 1. The table shows the ML model used, coordination type, system model, and the limitations of each approach.

2.4. Our Contribution

Most existing research on Co-BF is mainly focused on increasing beamforming quality for optimized signal transmission and reception. This quality improvement is related to proper beam alignment, reducing beam training overhead, and boosting the beam selection processes. Meanwhile, these studies often overlook the important aspect of intelligently nulling interference towards non-associated stations in overlapping service areas, which becomes important in dense wireless environments. Most beamforming approaches are based on predefined codebooks or channel knowledge – these assumptions are unfit for dynamic network environments. Galati-Giordano et al. [59] explained the key features of Wi-Fi 8 and mention that managing interference through nulling is critical, particularly in OBSS. They also suggest that null steering should be handled dynamically as the interference direction changes with station mobility.

Our work goes beyond these traditional approaches by explicitly introducing multi-AP coordination, intelligently deciding interference directions, and dynamic beamforming in ultra-dense Wi-Fi environments. Specifically, our method takes into account the mobility of stations and co-channel interference. Moreover, this work introduces an RL-based intelligent null steering framework that dynamically identifies and suppresses the strongest interference direction in dense multi-AP networks, overcoming the fundamental limitation of traditional beamforming (where N_t antennas can null at most $N_t - 1$ AP interference directions). By prioritizing dominant interference sources using real-time RL optimization, the system achieves near-optimal interference mitigation even in overloaded scenarios, while maintaining robust beamforming gain to the desired user. This approach bridges the gap between theoretical null-steering bounds and practical deployments, enabling scalable coexistence in next-generation Wi-Fi.

We decided to use the deep deterministic policy gradient (DDPG) model to handle the interference direction dynamically in the most disruptive direction. DDPG has been successfully applied in wireless communications for dynamic power control in ultra-dense networks, and multi-resource allocation tasks due to its stability and ability to generalize in high-dimensional environments [60, 61]. Sumiea et al. [62] discuss that DDPG is effective in high-dimensional, continuous action spaces where precise, real-time decision-making is required and highlights DDPG's ability to learn deterministic policies, making it well-suited for applications such as robotics, autonomous control, and energy management. To the best of our knowledge, there is no research in the field of Wi-Fi 8 Co-BF and optimum null steering based on DDPG to avoid channel access contention, enable transmissions at full power, and reduce latency.

3. System Model

In this work, we model a multi-AP Wi-Fi 8 environment where APs are positioned in fixed locations within the network. All APs operate on the same channel (OBSS conditions) using the full available spectrum, i.e., APs share the same frequency resources, which can lead to increased interference if not managed properly. Each AP is equipped with a uniform linear array (ULA) with N_t antenna elements, allowing for advanced beamforming and null steering capabilities (Figure 1). For simplicity, we assume all ULAs are mounted with a common horizontal orientation, so that beam angles are defined consistently across all APs. Stations associated with each AP are randomly distributed and move according to the random waypoint (RWP) model, which, unlike simpler mobility models, allows users to pause before moving again [63]. In the modeled wireless network, the Co-BF and nulling protocol are designed to optimize the signal quality at each station while minimizing interference from neighboring

APs and their stations, commonly known as OBSSs. The most relevant parameters used in the proposed coordinated Wi-Fi network are summarized in Table 2.

The stations move within a 10 m radius and change their position every 50 ms to achieve a human walking speed of 1.4 m/s [64]. In mobile scenarios, the channel measurement rate should scale with the speed of the station to ensure that CSI remains up to date. We assume channel measurements every 100 ms, which is a reasonable coherence interval at typical walking speeds and 5 GHz carrier frequency [65]. This temporal mismatch between stations changing position every 50 ms and channel measurements every 100 ms, causes the available CSI to become outdated, leading to decisions being made based on aged channel information. Channel estimation is performed during the sounding process, where the AP transmits known pilot symbols and the receiver observes the channel-affected signal. The received signal at the station is modeled as

$$\mathbf{y} = \mathbf{H}\mathbf{x} + \mathbf{n}, \tag{1}$$

where $\mathbf{x}$ is the transmitted pilot vector, $\mathbf{H}$ is the channel matrix to be estimated, and $\mathbf{n}$ is the additive white Gaussian noise. Based on this, the station computes the CSI and feeds it back to the transmitter. This CSI enables the transmitter to apply beamforming and interference nulling techniques, optimizing signal transmission based on real-time channel conditions. Maximizing the signal at the intended receiver requires optimal beamforming, an optimization problem that lacks a straightforward closed-form solution like null steering and is challenging to solve in practical scenarios with time-varying channels.

Using the obtained CSI, we design a beamforming strategy that maximizes the desired signal while nulling interference from unintended stations. To achieve the beamforming and null steering capabilities to get the highest possible throughput at station k, we design the beamforming weight vector $\mathbf{w}$ in the environment as

$$\mathbf{w} = \left(\mathbf{H}\mathbf{H}^H\right)^{-1} \mathbf{H}^H \mathbf{e}. \tag{2}$$

Here, the matrix $\mathbf{H}$ consists of the channel vector of the intended receiver along with channel vectors of unintended directions corresponding to neighboring stations that are to be nulled to mitigate interference. $\mathbf{H}$ captures how the signal propagates between the AP's antennas and the receiving stations. This zero-forcing formulation aligns the beam toward the intended station while nulling interference toward selected users, provided that $N_t \geq N_u$. In conventional beamforming approaches that require the number of antennas N_t to be greater than or equal to the number of users N_u, our system does not directly impose this constraint. Since we adopt our IntelliNull strategy, the agent learns to identify and null only the most critical interference directions from a larger set of potential interferes. As a result, even when $N_u > N_t$, the system remains feasible by selecting $N_u' \leq N_t$ dominant interference directions for nulling, while reserving one spatial DoF for beamforming toward the intended station.

To ensure compliance with the transmit power constraint, the resulting beamforming vector $\mathbf{w}$ is normalized such that $\mathbf{w} \leftarrow \mathbf{w}/\|\mathbf{w}\|$, ensuring unit norm beamforming weights, which can then be scaled appropriately to meet the AP's transmit power constraint. $\mathbf{H}$ is defined as

$$\mathbf{H} = \left[\mathbf{h}_1, \mathbf{h}_2, \ldots, \mathbf{h}_{N_u'}\right], \tag{3}$$

and the selection vector $\mathbf{e}$ is defined as

$$\mathbf{e}^T = [1, 0, 0, \ldots, 0], \tag{4}$$

where each $\mathbf{h}_i$ is an $N_t \times 1$ channel vector. Thus, the matrix $\mathbf{H}$ has dimensions $N_t \times N_u'$, where N_u' is a subset of N_u and represents the number of stations being considered for beamforming and nulling (i.e., the intended station and the interfering ones). This formulation allows to design a beamforming vector $\mathbf{w}$ such that $\mathbf{H}^H\mathbf{w} = \mathbf{e}$, where the first element of $\mathbf{e}$ is 1 (for the intended user), and the rest are 0 (to null the others). This vector $\mathbf{e}$ ensures that the beamforming vector aligns with the desired station channel while selectively nulling interference from other sources.

To minimize interference at unintended receivers, we form the matrix $\mathbf{H}$ by combining the channel vectors $\mathbf{w}$ obtained from the propagation environment, arranging them to place the intended receiver first, followed by vectors representing interference directions to be nulled. $\mathbf{H}^H$ denotes the Hermitian transpose (complex conjugate transpose) of $\mathbf{H}$, which is used in the least-squares formulation to solve for the optimal beamforming vector. In the expression $(\mathbf{H}\mathbf{H}^H)^{-1}\mathbf{H}^H$, the Hermitian transpose ensures proper handling of the complex-valued channel matrix, allowing us to accurately project the signal into the desired spatial directions while nulling interference. To further enhance robustness in practical wireless environments, where the channel matrix $\mathbf{H}$ can become ill-conditioned or lose rank due to mobility, fading, or interference, we use the Moore-Penrose pseudo-inverse instead of the regular inverse. This approach ensures that the beamforming vector $\mathbf{w}$ remains stable and reliable even under dynamic or noisy conditions.

The total transmit power $P_{tx,i}$ radiated by an AP_i is set to 20 dBm. The power of the transmitted signal reduces as it travels due to path loss. To capture real-world attenuation, we combine free space path loss (FSPL) with shadowing, which represents signal attenuation due to distance in free-space conditions. FSPL is computed using the distance between transmitter and receiver and the signal frequency, allowing proper modeling of large-scale propagation effects. So, a path loss model is used in this experiment by following the Friis transmission equation

$$\mathrm{PL}_{\mathrm{fs}}(d) = 20 \cdot \log_{10}\left(\frac{4\pi d f}{c}\right), \tag{5}$$

where d is the distance between the transmitter and receiver, f is the carrier frequency which is 5 GHz, and c is the speed of light. To account for real-world obstructions, we augment free-space path loss FSPL with log-normal shadowing such as

$$\mathrm{PL}(d) = \begin{cases} \mathrm{PL_{fs}}(d) + n, & \text{if } d \le 10, \\ \mathrm{PL_{fs}}(10) + 10 \cdot 3.5 \cdot \log_{10}\left(\frac{d}{10}\right) + n, & \text{if } d > 10. \end{cases} \tag{6}$$

Here, n represents the shadowing term, which follows a log-normal distribution $n \sim \mathcal{N}(0, \sigma^2)$. In our work, we set $\sigma^2 = 2$, to model log-normal shadowing effects typical of indoor environments (e.g., office spaces with partitions and furniture), striking a balance between realism in channel variations and stability for the learning process. This value aligns with empirical measurements from indoor wireless propagation studies [66]. FSPL is applied up to a distance of 10 m, and after that, a log-normal loss, with exponent 3.5, is added to simulate walls and objects the signal could pass through. We also model small-scale fading using Rician fading, which characterizes environments with a dominant line of sight (LOS) component (e.g., from beamforming) alongside multiple weaker scattered paths. The total signal power P at a receiver is defined as

$$P_{\mathrm{rx},k} = P_{\mathrm{tx},i} \cdot 10^{-\mathrm{PL}(d)/10} \cdot \left|\mathbf{h}_{i,k}^{H}\mathbf{w}\right|^2, \tag{7}$$

where $P_{\mathrm{tx},i}$ is the transmitted power and $\mathrm{PL}(d)$ is the path loss, which is converted to linear scale using $10^{-\mathrm{PL}(d)/10}$. $\mathbf{h}_{i,k}$ is the channel vector from the associated AP_i to station k, and $\mathbf{w}$ is the beamforming vector. The received signal strength is calculated using the absolute square of the inner product between the conjugate transpose of the channel vector and the beamforming vector, capturing the beam alignment gain by using $\left|\mathbf{h}_{i,k}^{H}\mathbf{w}_i\right|^2$. The total interference power at station k is obtained by summing contributions from all interfering APs as

$$P_{\mathrm{int},k} = \sum_{j \ne i} P_{\mathrm{tx},j} \cdot 10^{-\mathrm{PL}(d_{j,k})/10} \cdot \left|\mathbf{h}_{j,k}^{H}\mathbf{w}_j\right|^2, \tag{8}$$

where $P_{\mathrm{tx},j}$ is the transmit power of the interfering AP_j (with $j \ne i$), $\mathrm{PL}(d_{j,k})$ is the path loss from AP_j to station k (converted to linear scale), $\mathbf{h}_{j,k}$ is the channel vector from AP_j to station k, and $\mathbf{w}_j$ is the beamforming vector of AP_j. The term $\left|\mathbf{h}_{j,k}^{H}\mathbf{w}_j\right|^2$ represents the effective gain of the interfering signal received by station k due to AP_j.

The SINR provides a measure of the quality of the desired signal relative to both the noise and the interference from other overlapping networks, which is essential in evaluating network performance, especially in densely deployed wireless environments. The SINR at station k is calculated as

$$\mathrm{SINR}_k = \frac{P_{\mathrm{rx},k}}{P_{\mathrm{int},k} + P_{\mathrm{noise}}}, \tag{9}$$

where $P_{rx,k}$ represents the received signal power from the intended AP (transmitter) after antenna precoding, $P_{int,k}$ is the interference power from unintended transmitter within the OBSS. P_{noise} is the noise power, including thermal noise and any other background noise at the receiver. We account for thermal noise influenced by the channel bandwidth B and temperature. At room temperature, the thermal noise is approximately −174 dBm, and it is scaled according to the channel bandwidth. The noise component also includes the receiver noise figure, which we set to 7 dB, consistent with the setup in [10]. The total noise power is calculated as:

Parameter	**Value**
Frequency band	5 GHz
Channel bandwidth	80 MHz
Noise figure	7 dB
Thermal noise at room temperature	−174 dBm
stations mobility	1.4 m/s
Time slot	50 ms
CSI acquisition interval	100 ms
Max. radius station to AP	10 m
Max. transmit power	20 dBm
Pathloss model	FSPL

Table 2: Wireless communication parameters

$$P_{\mathrm{noise}} = -174 + 10 \cdot \log_{10}(B) + 7. \tag{10}$$

The corresponding maximum amount of bits transmitted during the allocated T_{slot} is

$$\mathrm{R}_k = T_{\mathrm{slot}} \cdot B \cdot \log_2(1 + \mathrm{SINR}_k), \tag{11}$$

where T_{slot} represents the allocated time slot duration for each user within the network (without loss of generality, we use a slot time of $T_{\mathrm{slot}} = 50$ ms and a bandwidth of the wireless channel of $B = 80$ MHz). While this equation gives the total number of bits transmitted, the rate can be derived by dividing the result by the time slot duration. A critical aspect of the modeled wireless network is the dynamic movement of stations. The dynamic scenario is best suited for optimal evaluation of Co-BF. This movement simulates real-world dynamics where users are mobile, providing a realistic scenario for evaluating the performance of Co-BF.

The complete system architecture is depicted in Figure 2. There are two main parts: the RL agent (central controller) part and the environment (Wi-Fi network) part. The agent acts as a central controller that makes decisions for the Wi-Fi network. The beam angle (main lobe direction from the AP to its associated station) and path loss measurements are collected from each AP in the network environment. The calculated beam angles and path losses of each station with respect to their APs are passed as a state to the central controller every 50 ms. The RL agent's actor takes this state (observation) as input and decides which directions to null. The decision is then passed to each AP in the network part. The network part consists of APs, each serving a set of associated stations. Each AP beams toward its associated stations while nulling interference toward critical non-associated stations to improve the overall network

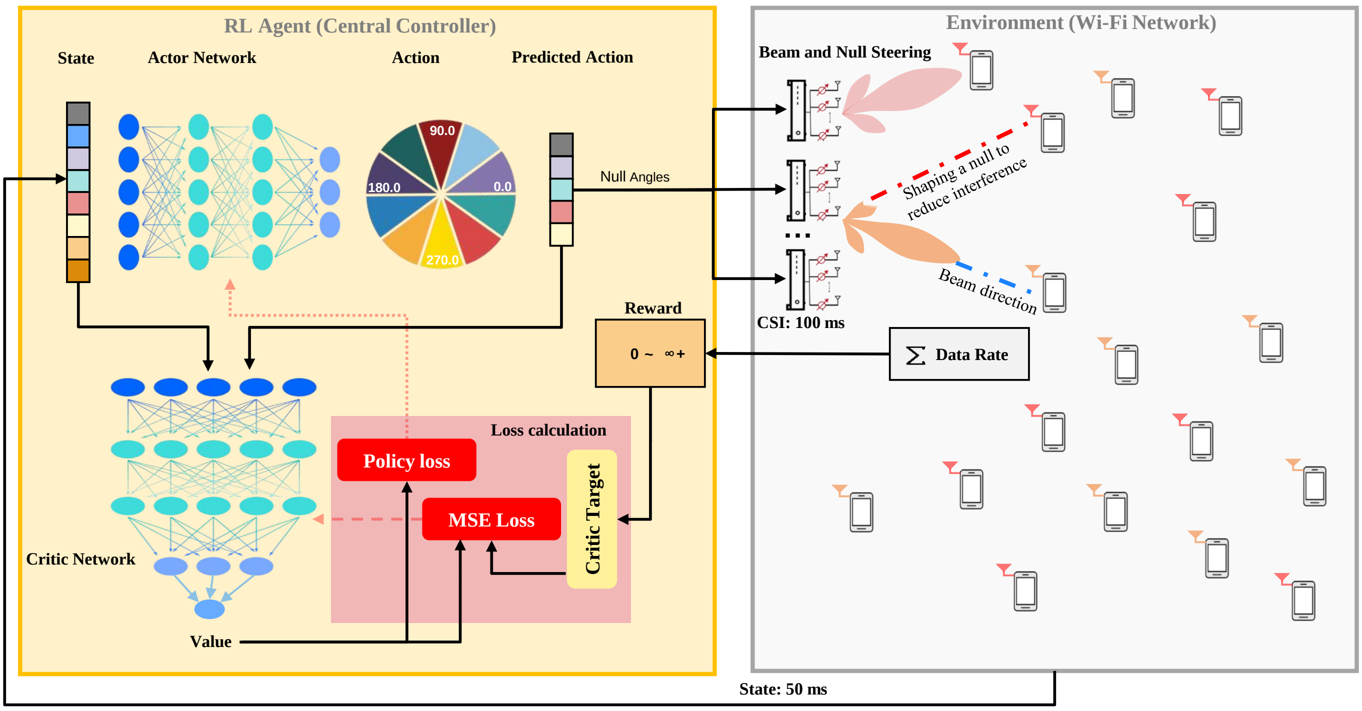

Figure 2: Proposed RL-based architecture for nulling configuration and Co-BF

performance. The aggregate sum of the throughput across the network is calculated and provided as feedback to the RL agent. The state is also fed into the critic network, which outputs a value. We then calculate the mean square error (MSE) between the value and the feedback value (reward). This process is repeated iteratively to minimize the MSE as much as possible. It is important to note that with each MSE calculation, the system updates the policy of the actor network, leading to better decisions and, consequently, improved overall network performance.

Furthermore, we assume that channel access is slotted and synchronized across all OBSSs. In our system model, basic service sets (BSSs) are assumed to operate in the same time slot, a synchronization achieved through mechanisms like the time synchronization function (TSF) [67]. This assumption aligns with MAPC principles, where APs are triggered to transmit simultaneously following a coordinated trigger frame (TF).

4. Reinforcement Learning-based Algorithm for Nulling Configuration

In the following, we explain the RL agent's interaction with the system model. Unlike other approaches that focus solely on beamforming optimization, IntelliNull emphasizes effectively directing beams toward associated stations while suppressing interference toward unintended recipients, including stations in neighboring BSSs in multi-AP environments. We use a DDPG model for this purpose. DDPG is an algorithm, used in RL, specifically designed for environments with continuous action spaces. It combines elements from both policy-based and value-based approaches, leveraging the strengths of DQN and deterministic policy gradient (DPG) to effectively handle continuous control tasks [68]. In this approach, the action space consists of possible null steering angles that the agent can predict for each AP to optimize the network performance. Training environments that have continuous observation and action space is challenging. However, with continuous values, the agent can find the best possible directions where the agent finds it better to predict the null angle. In a discrete action space, the agent is restricted to a limited set of predefined directions, which may cause it to miss potentially optimal values that lie between two discrete values. In contrast, a continuous action space allows the agent to explore the full range of directions without such limitations.

As per Algorithm 1, first, the RL agent is initialized with random weights, learning rate, and buffer. All APs have collected CSI from their stations through periodic channel sounding using Equation (1). The resulting path loss and angle information to each station is then combined to construct the observation space, which serves as the agent's representation of the current environment. Based on this observation, the agent selects nulling actions to suppress the most critical interference directions. The observation space is structured as

$$s = \{(\phi_0, PL_0)\}, \{(\phi_1, PL_1), \ldots, (\phi_{M_{\text{OBSS}}}, PL_{M_{\text{OBSS}}})\}, \tag{12}$$

where M_{OBSS} represents the number of OBSSs. The first two values in the observation correspond to the associated

Algorithm 1 IntelliNull platform for angle prediction

1: Initial DDPG: random weights for actor and critic; target actor and critic networks with weights θ_{μ^-} and θ_{Q^-} initialized to θ_μ and θ_Q; experience replay buffer $\mathcal{D}$; learning rate α
2: **for** each time slot **do**
3: 1. **Agent Interaction:**
4: i. Obtain stations angles and path loss around APs
5: ii. Update current observation space s_t
6: iii. Predict action a_t according to policy $\mu(s_t|\theta_\mu) + \mathcal{N}_t$ (where $\mathcal{N}_t$ is exploration noise)
7: iv. Execute action a_t by steering beam and null
8: v. Calculate received power, SINR, and reward r_t, and next state s_{t+1}
9: vi. Store transition (s_t, a_t, r_t, s_{t+1}) in experience replay buffer $\mathcal{D}$
10: 2. **Update Agent Networks:**
11: i. Sample random mini-batch of transitions from $\mathcal{D}$
12: ii. For each transition (s, a, r, s') in the mini-batch, compute target value:

$$y = r + \gamma Q(s', \mu(s'|\theta_{\mu^-})|\theta_{Q^-})$$

13: iii. Update critic network by minimizing loss:

$$L = \frac{1}{N}\sum_i (y_i - Q(s_i, a_i|\theta_Q))^2$$

14: iv. Update actor network by maximizing expected reward:

$$\nabla_{\theta_\mu} J \approx \frac{1}{N}\sum_i \nabla_a Q(s, a|\theta_Q)\Big|_{a=\mu(s|\theta_\mu)} \nabla_{\theta_\mu}\mu(s|\theta_\mu)$$

15: v. Update target networks:

$$\theta_{Q^-} \leftarrow \tau\theta_Q + (1-\tau)\theta_{Q^-}$$

$$\theta_{\mu^-} \leftarrow \tau\theta_\mu + (1-\tau)\theta_{\mu^-}$$

16: **end for**

station, which includes the angle ϕ from the AP_i to station k and the corresponding path loss PL. The remaining values in the observation represent the non-associated stations in the OBSSs, with their respective null angles and path losses. This observation representation allows the agent to consider interference from non-associated stations, which are often located in the vicinity of the AP but are not directly connected. These non-associated stations can still interfere with the associated stations signal, and the agent must optimize null steering. After collecting the observation space s_t, the agent can predict all possible or maybe a few of the null angles, depending on how much that decision can improve the reward. Based on these actions a_t, APs generates antenna weights for the ULAs using Equation (2). The idea is to steer nulls toward directions where OBSS stations are located while focusing the main beam toward its currently served station by directing the signal power $P_{tx,i}$.

After directing the signal power the stations calculate the received power using Equation (7) and the interference for each interfering stations using Equation (8). The SINR is calculated at each station using Equation (9) and then the throughput as a reward using Shannon capacity in Equation (11). The sum of the throughput is fed back to the RL agent in the form of a reward r_t and the next state s_{t+1} of the environment. These observations are stored in the replay buffer $\mathcal{D}$ for off-policy training, where mini-batches of transitions (s_t, a_t, r_t, s_{t+1}) are sampled to update the agent's policy and value networks.

After each interaction with the environment (lines 10–16 in Algorithm 1), a mini-batch of past experiences is randomly sampled from the replay buffer $\mathcal{D}$. For each transition, the target Q-value y is computed using the target networks (μ^- and Q^-), which helps stabilize training. Back-propagation is also considered in the DDPG network and the MSE is calculated for each Q-value produced using the loss function

$$L_{\text{critic}} = \text{MSE}(Q_{\text{current}}, Q_{\text{target}}). \tag{13}$$

The weights of each network are implicitly updated based on the loss corresponding to its allocated portion of the reward. This reward decomposition, like Q-value prediction, is learned over time through experience. Next, the actor network is updated using the policy gradient derived from the critic, which encourages actions that yield higher rewards. Finally, both the actor and critic target networks are softly updated by blending their parameters with the current networks using a small update factor, ensuring smoother and more stable learning. This update process allows the agent to iteratively refine its nulling strategy based on observed network dynamics.

In our IntelliNull system, the agent tries many different actions to maximize the overall throughput. The agent intelligently steers null interference from specific directions that would most affect the system's performance. By using throughput as the reward function, the agent is encouraged to only null interference in those directions that enhance the overall rate. This ensures that the agent adapts its nulling strategy to maximize system performance, rather than randomly nulling all interference. The reward function guides the agent's learning process, and in the final stage, the agent's policy converges to those actions that can maximize its cumulative reward.

The parameters for actor-critics networks and Ornstein-Uhlenbeck (OU) noise are gathered in Table 3. The architecture of the actor network was chosen to balance complexity and computational efficiency. The three hidden layers with 400 and 300 neurons provide sufficient capacity to learn complex nonlinear mappings from the input

Parameter	Value
Action space size	Dep. on netw. topology
State space size	Dep. on netw. topology
Actor / critic hidden layers	[400, 300]
Buffer capacity	100,000 samples
Actor learning rate	0.0001 step/iteration
Critic learning rate	0.001 step/iteration
Optimizer	Adam
Loss function	MSE
Discount Rate	0.99
Batch size	1024
OU λ	0.9995
OU τ	0.001
OU σ	0.20
OU θ	0.15
OU μ	0.0
OU s_{OU}	1.0

Table 3: Actor-critic parameters

state space to the action space, which is crucial for the high-dimensional problem of beamforming and null steering. ReLU activation functions enable efficient gradient propagation, reducing the vanishing gradient issue. The hyperbolic tangent (TanH) activation function at the output layer ensures bounded outputs, matching the range of valid null angles. The TanH activation function ensures that the output action values are normalized, making them suitable for continuous control tasks. The observation space is normalized between 0 and 1. The action space is normalized between -1 and 1, allowing the RL agent to operate within a continuous actions space. The critic network evaluates the quality of the action taken by the actor network by estimating the expected return Q-value given the current state and action. This network is similar in structure to the actor network but includes both the state and action as inputs.

State and action spaces are based on the specific Wi-Fi network topology. If the Wi-Fi network topology increases, the state and action space also increase to ensure that the agent can make better decisions for that specific topology. The actor-critic learning rates are 0.0001 and 0.001, respectively, with a buffer size 100000, and a batch size of 1024 to allow the agent to learn from different past experiences in a complex environment. We use the Adam optimizer [69], which is well suited for problems that are large in terms of parameters, easy to implement, and computationally efficient. Lillicrap et al. [68] proposed that the combination of the OU process, soft update parameter τ, decay parameter λ, magnitude of the diffusion term σ, magnitude of the drift term θ, initial scaling factor s_{OU}, and mean of the noise process μ, can help the actor and critic networks in the continuous control environment to balance the learning stability and asymptotic mean of the noise process which controls the mean value of the noise for exploration in the actions.

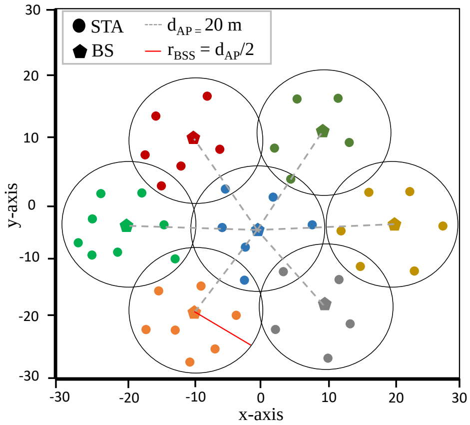

Figure 3: Example network topology as used on our simulations

5. Performance Evaluation

5.1. Simulation Setup

We developed a Co-BF simulator in Python. The setup consists of a custom number of APs, each equipped with a custom number of antennas. The number of antennas directly impacts the beamforming and null steering capabilities of each AP. Stations move within a 10 m radius, mimicking the movement of users in an office or home environment. A minimum distance between stations and APs of 1.5 m is set to avoid singularities in path loss calculations. We explore network topologies with a variable number of APs, number of antennas per AP, and users (stations). Figure 3 depicts an exemplary network topology consisting of seven APs with five to seven stations per AP and the circles represent the radius of each AP, where the stations can possibly move.

For the performance comparison of our IntelliNull-based solution, we also implemented an *Oracle* approach, in which a custom agent operates assuming perfect CSI, meaning it has full knowledge of the wireless environment at any given moment in time. This agent is pre-programmed with precise beamforming and null-steering angles that maximize throughput and minimize interference, ensuring optimal performance. The Oracle provides an ideal performance benchmark for the IntelliNull system by assuming perfect channel knowledge.

5.2. Comparison with State of the Art

To further evaluate the effectiveness of IntelliNull, we compare its performance against the nulling strategy introduced by Galati-Giordano et al. [59], representing a state-of-the-art (SOTA) method adopted in IEEE 802.11bn evaluations, as well as random nulling, which randomly allocates nulling directions within available spatial DoF.

In this first experiment, we adopt the same topology and key parameters, for example, number of APs, number of antennas per AP, stations associated per AP, and bandwidth, to enable a direct comparison. In particular, we use two APs operating in the 6 GHz band using a 160 MHz channel and a time slot of 50 ms. Each AP is equipped

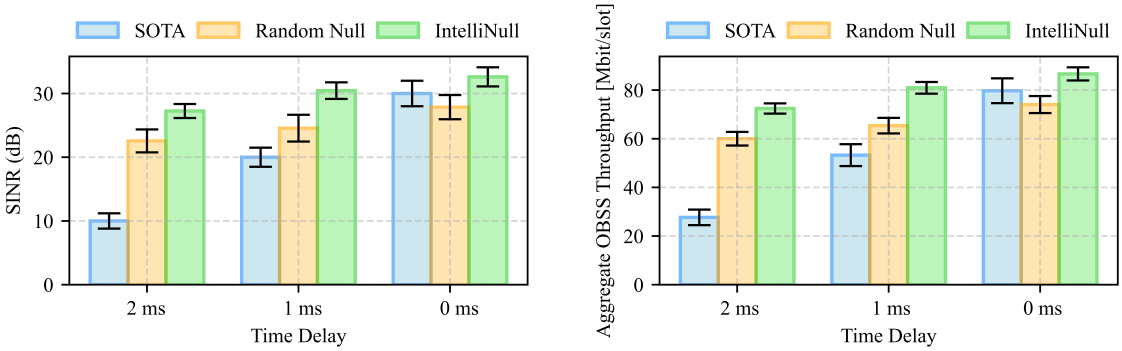

(a) SINR

(b) Throughput

Figure 4: Comparison of nulling strategies: SOTA, null random angles, and null angles from RL agents.

with four antennas and one associated station. The CSI acquisition delay, representing the time required to gather and process CSI, is varied from 0 ms to 2 ms to reflect realistic overhead scenarios. AP locations are fixed at (5 m, 10 m) and (10 m, 10 m), while their associated stations are positioned at (5 m, 12.5 m) and (10 m, 12.5 m), respectively. All methods are evaluated under identical conditions to ensure a fair comparison.

Results in Figure 4 show that the DDPG-based IntelliNull agent observes CSI-derived channel metrics and interference patterns and learns a nulling policy that maximizes aggregate throughput and SINR. Instead of relying on fixed rules, the agent dynamically selects the most impactful interference directions to null, adapting to mobility and CSI aging in real time. Specifically, with fresh CSI (i.e., 0 ms time delay), IntelliNull achieves an SINR of over 32 dB and throughput exceeding 85 Mbit. Even under 2 ms delay, it maintains robust performance, whereas SOTA and random nulling degrade significantly, with SOTA showing a steep drop to 10 dB SINR and only 28 Mbit throughput from 0 ms to 2 ms CSI delay, SOTA performance degrades by over 20 dB in SINR and nearly 60 Mbit in throughput, while IntelliNull maintains high performance with less than 5 dB SINR and 15 Mbit throughput loss, demonstrating stronger resilience to outdated CSI. Unlike random nulling that assigns null directions arbitrarily, IntelliNull learns to prioritize the most critical interference directions using RL, leading to smarter null allocation and better spatial reuse.

These results highlight two key insights. Firstly, although random nulling uses all available DoF but lacks spatial selectivity and often nulls non-critical interference directions, leading to modest gains and high variance. Secondly, while SOTA provides significant benefits under perfect or near-perfect CSI, its performance degrades with increasing delay due to the lack of adaptivity. In contrast, IntelliNull's RL-driven strategy learns to prioritize and steer nulls toward the most disruptive interference paths, achieving resilient interference suppression even with imperfect CSI. This confirms the potential of RL-based null steering to enhance both spatial reuse and reliability under practical overhead constraints in ultra-dense Wi-Fi deployments. All results are averaged over multiple randomized runs, and error bars in the figures indicate standard deviation, confirming the statistical reliability of the observed performance trends.

5.3. Beamforming vs. Beamforming Plus Null Steering

Next, we study the impact that null steering adds to beamforming. Figure 5 illustrates the effect of beamforming and null steering on the aggregate OBSS throughput for a scenario where we have two APs and each AP has one connected station. Figure 5a shows the results without null steering with a 10 dB antenna gain for both AP_A and AP_B as a baseline. As the baseline experiment, we only use beamforming without nulling. In Figure 5c, null steering is added where the black dash line is the null steering directed towards the interference with 8.98 dB for AP_A and 9.79 dB for AP_B reduction in antenna gain. In both figures, the station with the blue antenna indicates the associated station (STA_{ASST}) to their APs, while the stations with the red antenna represents the direction of the interference station (STA_{INT}) for each AP. As shown in Figure 5d, even with the reduction of the antenna gain, the throughput is consistently higher when null steering is applied.

By directing nulls toward neighboring receivers (i.e., stations associated with other APs), APs reduce the interference, thereby enabling more efficient communication with the associated station. In contrast, Figure 5b shows lower throughput due to increased interference from neighboring devices and only beamforming. As the stations are continuously moving, throughput is good from 0 to 100 seconds for both cases. However, an interesting observation occurs when the associated STA_{ASST} and the interference STA_{INT} are in almost the same direction while moving around their AP, as shown in our example for AP_A. In this case, the throughput drops significantly in both cases between 100 and 175 seconds.

However, with beamforming plus null steering, the degradation is around 80 Mbit and is noticeably less severe compared to the scenario with only beamforming where the throughput drops to around 20 Mbit. This is due to the

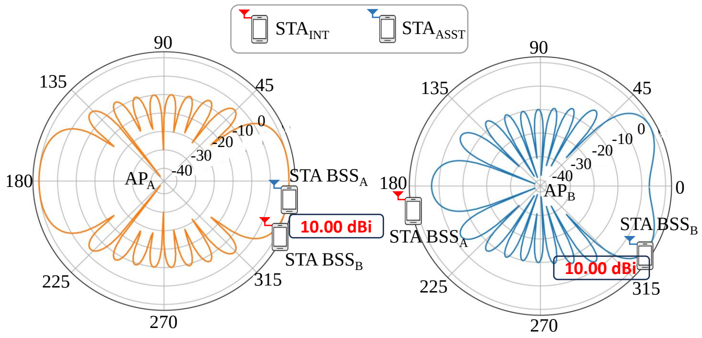

(a) Beam and side lobes (only beamforming)

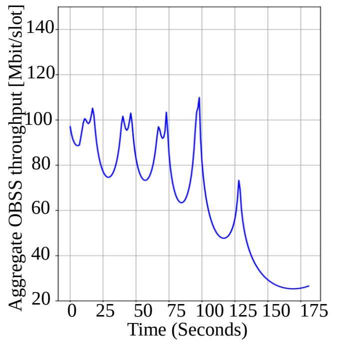

(b) Throughput (only beamforming)

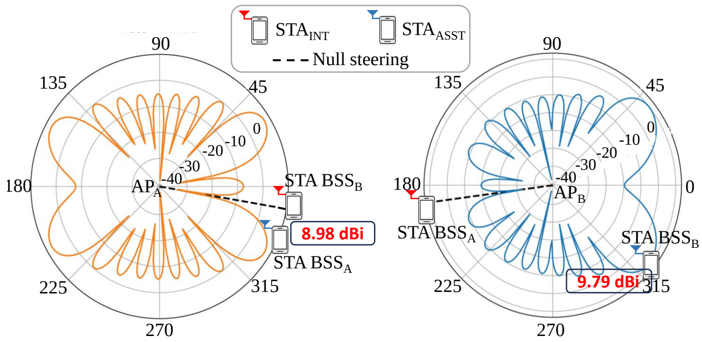

(c) Beam and side lobes (beamforming plus nulling)

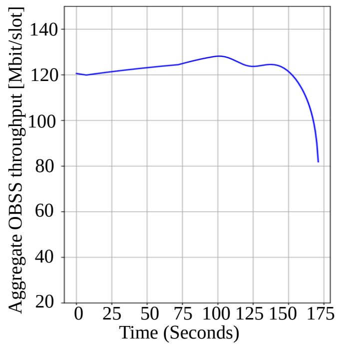

(d) Throughput (beamforming plus nulling)

Figure 5: Comparison beam construction and achieved throughput.

mobility of stations (Figure 6), for which at some points in space beamforming only cannot generate optimal channel conditions. This effectively demonstrates the benefits of null steering in mitigating interference even in challenging conditions and even with the reduction in gain in the main beam lobe. These results highlight the effectiveness of null steering in reducing interference and maintaining robust communication in dynamic environments with interfering stations, especially when the associated stations and interfering directions are in the same direction.

5.4. Impact of APs, Stations, and Antennas

We first analyze the performance of our IntelliNull platform in comparison to the theoretical Oracle and a Baseline approach. Different experiments are conducted to evaluate

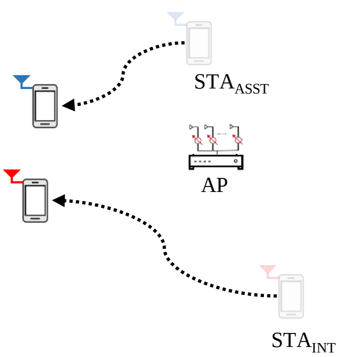

Figure 6: Stations mobility around the APs

the effectiveness of IntelliNull across different scenarios, varying the number of antennas, APs, and stations. We present selected results in Figure 7, where the background, pale-colored curves show the average throughput while the foreground, intense-colored curves represent the moving average (with a window size of 15), illustrating both the performance of our algorithm and its convergence time. The episodes are the number of iterations the RL agent interacts with the network environment. In simple scenarios with only one station, the IntelliNull approach converges quickly to a level that is close to the Oracle. As can be seen in Figures 7a to 7c, the convergence rate is even almost independent of the number of antennas used at the AP. Of course, the overall performance improves significantly, if more antennas are available.

The situation is different with increasing complexity of the beamforming and nulling solution space. As shown in Figures 7d to 7f, the convergence time increases for IntelliNull when 15 stations need to be considered. In these figures, also the number of antennas at the AP is increases from 4 to 10. Figure 7f shows the most extreme case (15 stations, 10 antenna). This smoothing was applied solely in each plot for clear visualization. The convergence was observed after approximately 100 episodes for Figures 7a to 7c, where the total number of moving stations was 7, and after approximately 230 episodes for Figures 7d to 7f, where the total number of moving stations was 105. The average sum rate stabilizes with minimal fluctuations.

In all cases, the baseline, which represents only beam-

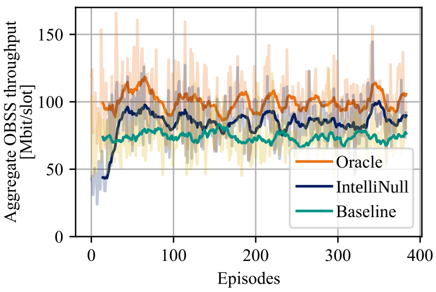

(a) 7 APs, 4 antennas, 1 station

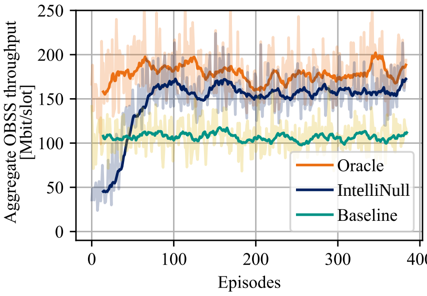

(b) 7 APs, 6 antennas, 1 station

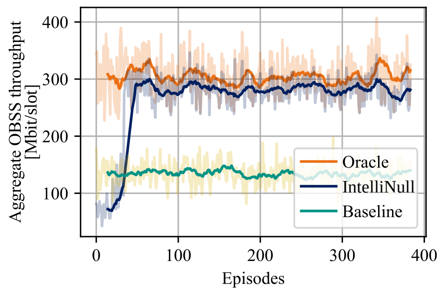

(c) 7 APs, 10 antennas, 1 station

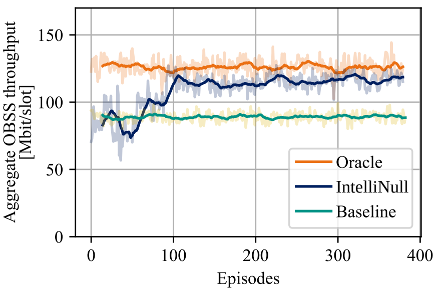

(d) 7 APs, 4 antennas, 15 station

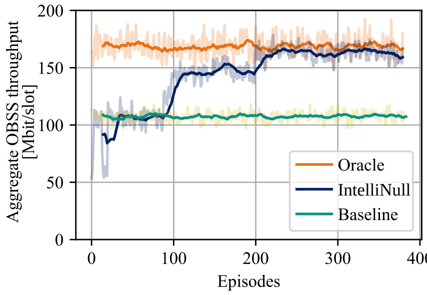

(e) 7 APs, 6 antennas, 15 station

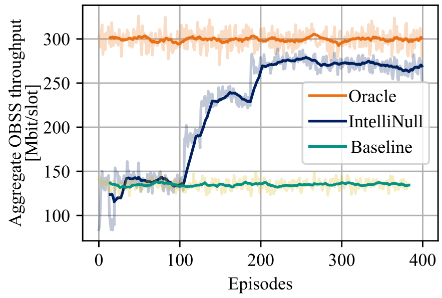

(f) 7 APs, 10 antennas, 15 station

Figure 7: Convergence of IntelliNull (DDPG) and its steady state performance compared to Oracle across different configurations of the number of stations and antennas per AP.

forming without null steering, performs worse than both the IntelliNull approach and the Oracle. This highlights the importance of using both beamforming and null steering for effective interference mitigation. Despite the convergence time, our ML-based solution still achieves close to optimal results (represented by the Oracle solution).

5.5. Performance Gap

Beyond the absolute performance results, we are also interested in how closely our algorithm matches the Oracle. The performance gap $\frac{|\text{Oracle Reward} - \text{IntelliNull Reward}|}{\text{Oracle Reward}}$ between the rewards by the IntelliNull system and the Oracle approach across all experiments follows a consistent pattern as shown in Figure 8. Initially, the performance gap is relatively high, reflecting the early learning stages of our algorithm. As time progresses, there is a sharp decline in the performance gap, which stabilizes at very low values, typically around 10–15 % across different configurations of antennas and stations. This trend indicates that the IntelliNull system rapidly learns to approximate the optimal performance. However, the stabilized gap also exhibits minor fluctuations, particularly in more complex scenarios with higher numbers of antennas and stations, suggesting that while IntelliNull can achieve a performance close to the Oracle, it occasionally struggles with the added complexity (see, for example, Figure 8f).

5.6. Impact of Station Mobility

We further study the impact of mobility of the stations on the performance of our algorithm. All the experiments discussed so far included user mobility. If we keep the user stationary, the IntelliNull model achieves a relatively stable average sum rate, with few fluctuations and a performance that approaches that of the Oracle as shown in Figure 9a. This is because the characteristics of the wireless communication channel, such as signal strength, interference levels, and path loss, do not change significantly over time, which allows the Oracle to achieve the theoretic optimum and the IntelliNull model to learn and optimize the nulling angles effectively. The baseline, in contrast, represents a setup where only beamforming is performed without considering null steering. As a result, it consistently underperforms compared to both the Oracle and the DDPG-based IntelliNull model, as it lacks the additional degree of freedom provided by null steering. In Figure 9a, we observe that the baseline maintains a lower aggregate throughput compared to both Oracle and IntelliNull, reinforcing the significance of null steering in mitigating interference.

However, in general, due to mobility, the stations often face a low throughput because the null angle and the beam angle come in the same direction or almost in the same direction for APs time to time. Figure 9b shows a scenario where 50% of the stations are static and 50% are mobile. In this case, the throughput is higher for Oracle and IntelliNull compared to the scenario where all the stations are mobile Figure 9c but lower than the scenario where all stations are static Figure 9a. That shows that with mobility the network topology gets more complex and the interference increases with the mobility. Indeed, in Figures 9b and 9c, there are brief moments where IntelliNull

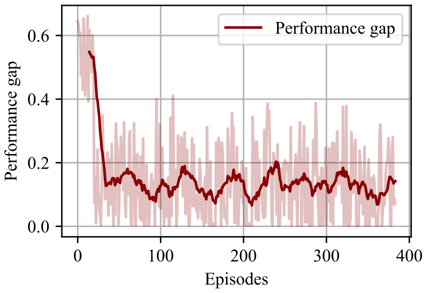

(a) 7 APs, 4 antennas, 1 station

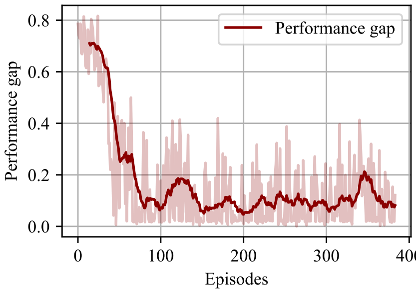

(b) 7 APs, 6 antennas, 1 station

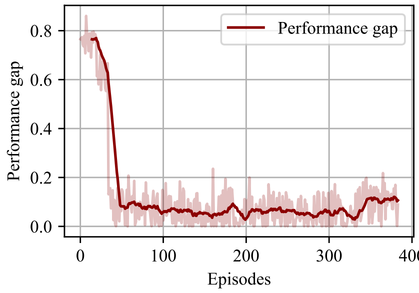

(c) 7 APs, 10 antennas, 1 station

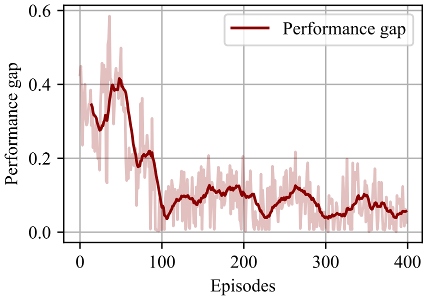

(d) 7 APs, 4 antennas, 15 stations

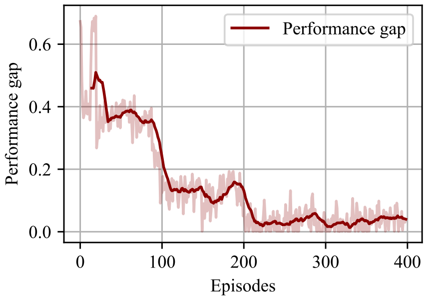

(e) 7 APs, 6 antennas, 15 stations

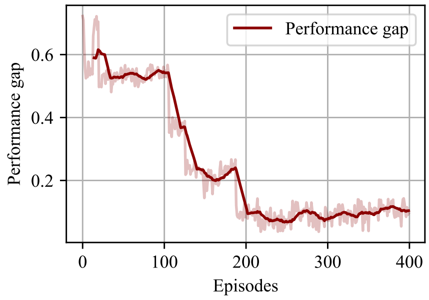

(f) 7 APs, 10 antennas, 15 stations

Figure 8: Performance gap between IntelliNull and Oracle across different configurations of number of stations and antennas per AP

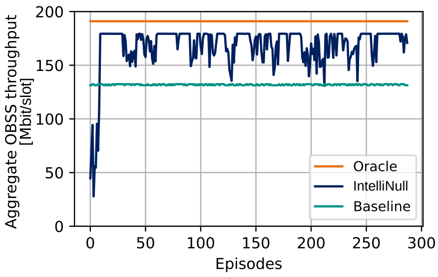

(a) Static

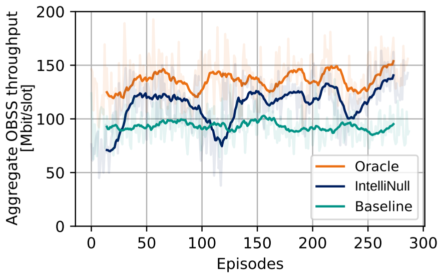

(b) 50% mobile

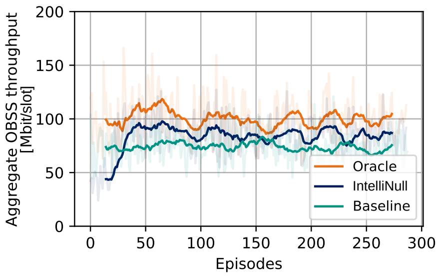

(c) 100% mobile

Figure 9: Impact of mobility in a scenario with 7 APs, 4 antennas per AP, and 1 station per AP.

performs slightly worse than classical beamforming. This occurs primarily during the initial learning or adaptation phases, particularly in highly dynamic scenarios where station mobility rapidly changes the interference landscape. This also occurs when the beam angle and the interference direction are nearly aligned, which affects the main lobe gain. This condition, where the beam and null angles are closely aligned, occurs frequently in the experiments shown in Figure 9c, where multiple APs with mobile stations operate in a dense environment. We also observe a moderate throughput drop and variability in Figure 9b compared to Figure 9a, as 50% of the stations are mobile while the remaining 50% are static. In contrast, in the fully mobile scenario of Figure 9c, the beam and null directions frequently overlap, leading to a significant throughput degradation and variability compared to Figures 9a and 9b. This beam and null angle alignment issue contributes to the performance gap observed between static and mobile deployments.

The baseline remains consistently lower in all mobility scenarios, as it does not leverage null steering to mitigate interference, making it more susceptible to the challenges introduced by user movement. This experiment is performed by considering 7 APs, 4 antennas, and 1 station per AP. This trend was expected, as mobility always increases the bit error rate [70].

6. Conclusion

We have explored the application of the IntelliNull platform to the problem of null steering in wireless communication networks, specifically within the context of Wi-Fi 8. The performance of our intelligent null steering by reinforcement learning (IntelliNull) approach was evaluated against an Oracle approach, which served as an ideal benchmark with perfect CSI and precomputed optimal null angles. Across all experiments, our intelligent null steering by reinforcement learning (IntelliNull) approach demonstrates a strong ability to learn and adapt to various configurations, progressively improving its performance over time.

In summary, we observed the following advantages (and limitations) of our IntelliNull approach:

(a) Beamforming vs. beamforming plus nulling: When comparing experiments with only beamforming and beamforming plus nulling, it was observed that beamforming plus nulling significantly improves the overall throughput. This emphasizes the effectiveness of null steering in enhancing network performance and minimizing interference.

(b) Optimal nulling vs. random interference nulling: We have shown that random nulling all possible interference directions does not produce the best overall sum throughput. The results show that nulling only the crucial interference directions leads to better network performance and higher throughput, highlighting the importance of intelligently selecting which interference directions to null rather than nulling all directions indiscriminately.

(c) CSI acquisition and optimization: The availability of accurate CSI data was found to be a critical factor in the performance. IntelliNull platform can adapt to make a close-to-perfect decision comparable to the theoretical Oracle performance.

(d) Mobility and interference: In mobility scenarios, the dynamic nature of interference presents a significant challenge. The results show that the IntelliNull platform can still adapt and make satisfactory decisions, indicating the superiority of DDPG application in Wi-Fi to find null direction over exhaustive search.

(e) Impact of antenna and user density: In simpler setups with few antennas and users, IntelliNull platform performs extremely well. As the number of antennas and stations increases, the convergence time of IntelliNull is higher.

In future work, we aim to further improve IntelliNull. Fluctuations observed in DDPG performance, particularly in early episodes, suggest that while the algorithm is effective, there is room for improvement of convergence time.

Acknowledgments

This work was supported by the Federal Ministry of Education and Research (BMBF, Germany) within the 6G Research and Innovation Cluster 6G-RIC under Grant 16KISK020K as well as by the German Research Foundation (DFG) and the Polish National Science Centre (NCN) within the project ML4WiFi under grants DR 639/28-1 and 2020/39/I/ST7/01457, respectively.

References

[1] Xiaoqian Liu, Tingwei Chen, Yuhan Dong, Zhi Mao, Ming Gan, Xun Yang, and Jianmin Lu. Wi-Fi 8: Embracing the Millimeter-Wave Era. *IEEE Communications Magazine*, 63(3):69–75, March 2025. ISSN 0163-6804. doi: 10.1109/mcom.002.2400059.

[2] Armed Tusha and Hüseyin Arslan. Interference Burden in Wireless Communications: A Comprehensive Survey from PHY Layer Perspective. *IEEE Communications Surveys & Tutorials*, pages 1–1, October 2024. ISSN 1553-877X. doi: 10.1109/comst.2024.3487068.

[3] Xuecheng Xie, Dongheng Zhang, Yadong Li, Yang Hu, Qibin Sun, and Yan Chen. Robust WiFi Respiration Sensing in the Presence of Interfering Individual. *IEEE Transactions on Mobile Computing*, 23(8):8447–8462, August 2024. ISSN 1536-1233. doi: 10.1109/tmc.2023.3348879.

[4] Erik G. Larsson, Ove Edfors, Fredrik Tufvesson, and Thomas L. Marzetta. Massive MIMO for next generation wireless systems. *IEEE Communications Magazine*, 52(2):186–195, February 2014. ISSN 0163-6804. doi: 10.1109/mcom.2014.6736761.

[5] Haris Gacanin and Amir Ligata. Wi-Fi Self-Organizing Networks: Challenges and Use Cases. *IEEE Communications Magazine*, 55(7):158–164, July 2017. ISSN 0163-6804. doi: 10.1109/mcom.2017.1600523.

[6] Meiping Peng, Bo Li, and Zhongjiang Yan. Multi-BSS Multi-User Full Duplex MAC Protocol based on AP Cooperation for the Next Generation WLAN. *ACM/Springer Mobile Networks and Applications*, 28(3):1019–1030, June 2023. ISSN 1383-469X. doi: 10.1007/s11036-023-02132-8.

[7] Shanzhi Chen, Ying-Chang Liang, Shaohui Sun, Shaoli Kang, Wenchi Cheng, and Mugen Peng. Vision, Requirements, and Technology Trend of 6G: How to Tackle the Challenges of System Coverage, Capacity, User Data-Rate and Movement Speed. *IEEE Wireless Communications*, 27(2):218–228, April 2020. ISSN 1536-1284. doi: 10.1109/mwc.001.1900333.

[8] Evgeny Khorov, Ilya Levitsky, and Ian F. Akyildiz. Current Status and Directions of IEEE 802.11be, the Future Wi-Fi 7. *IEEE Access*, 8:88664–88688, May 2020. ISSN 2169-3536. doi: 10.1109/ACCESS.2020.2993448.

[9] Toni Adame, Marc Carrascosa-Zamacois, and Boris Bellalta. Time-Sensitive Networking in IEEE 802.11be: On the Way to Low-Latency WiFi 7. *MDPI Sensors*, 21(15):4954, July 2021. ISSN 1424-8220. doi: 10.3390/s21154954.

[10] Adrian Garcia-Rodriguez, David Lopez-Perez, Lorenzo Galati-Giordano, and Giovanni Geraci. IEEE 802.11be: Wi-Fi 7 Strikes Back. *IEEE Communications Magazine*, 59(4):102–108, April 2021. ISSN 0163-6804. doi: 10.1109/mcom.001.2000711.

[11] Francesc Wilhelmi, Sergio Barrachina-Muñoz, Cristina Cano, Ioannis Selinis, and Boris Bellalta. Spatial Reuse in IEEE 802.11ax WLANs. *Elsevier Computer Communications*, 170: 65–83, March 2021. ISSN 0140-3664. doi: 10.1016/j.comcom.2021.01.028.

[12] Poorya Karami and Seyed Mojtaba Atarodi. Beamforming, null-steering, and simultaneous spatial and frequency domain filtering in integrated phased array systems. *AEU - International Journal of Electronics and Communications*, 110:152868, October 2019. ISSN 1434-8411. doi: 10.1016/j.aeue.2019.152868.

[13] Andreas F. Molisch, Vishnu V. Ratnam, Shengqian Han, Zheda Li, Sinh Le Hong Nguyen, Linsheng Li, and Katsuyuki Haneda. Hybrid Beamforming for Massive MIMO: A Survey. *IEEE Communications Magazine*, 55(9):134–141, 2017. ISSN 0163-6804. doi: 10.1109/mcom.2017.1600400.

[14] Xin Wang, Xiaolin HOU, Lan CHEN, Yoshihisa Kishiyama, and Takahiro Asai. Deep Learning-Based Massive MIMO CSI Acquisition for 5G Evolution and 6G. *IEICE Transactions on Communications*, 105(12):1559–1568, December 2022. doi: 10.1587/transcom.2022ebp3009.

[15] Gaurav Nigam, Paolo Minero, and Martin Haenggi. Coordinated Multipoint Joint Transmission in Heterogeneous Networks. *IEEE Transactions on Communications*, 62(11):4134–4146, November 2014. ISSN 1558-0857. doi: 10.1109/tcomm.2014.2363660.

[16] Ralf Irmer, Heinz Droste, Patrick Marsch, Michael Grieger, Gerhard Fettweis, Stefan Brueck, Hans-Peter Mayer, Lars Thiele, and Volker Jungnickel. Coordinated multipoint: Concepts, performance, and field trial results. *IEEE Communications Magazine*, 49(2):102–111, February 2011. ISSN 0163-6804. doi: 10.1109/mcom.2011.5706317.

[17] Zhao Li, Jie Chen, Zheng Lu, Cuiping Shao, Kang G. Shin, and Jia Liu. Coordinated Multi-Point Transmissions Based on Interference Alignment and Neutralization. *IEEE Transactions on Wireless Communications*, 18(7):3347–3365, July 2019. ISSN 1536-1276. doi: 10.1109/twc.2019.2908159.

[18] K.R. Kavitha and T. Sivakumar. A Comprehensive Survey on Beamforming and Antenna Selection in MIMO Systems Using Deep Learning and Machine Learning Techniques with Future Research Directions. In *2nd World Conference on Communication & Computing (WCONF 2024)*, pages 1–8, Raipur, India, July 2024. IEEE. doi: 10.1109/wconf61366.2024.10692227.

[19] Haya Al Kassir, Zaharias D. Zaharis, Pavlos I. Lazaridis, Nikolaos V. Kantartzis, Traianos V. Yioultsis, and Thomas D. Xenos. A Review of the State of the Art and Future Challenges of Deep Learning-Based Beamforming. *IEEE Access*, 10:80869–80882, 2022. ISSN 2169-3536. doi: 10.1109/access.2022.3195299.

[20] Jaber Kakar and Aydin Sezgin. A Survey on Robust Interference Management in Wireless Networks. *Entropy*, 19(7):362, July 2017. ISSN 1099-4300. doi: 10.3390/e19070362.

[21] A. D. Borah, Md. A. Hussain, and J. Bora. Analysis of Interference Alignment Based Multi-User MIMO Precoding. *Radioelectronics and Communications Systems*, 64(11):612–618, November 2021. ISSN 1934-8061. doi: 10.3103/s0735272721110054.

[22] Shikhar Verma, Tiago Koketsu Rodrigues, Yuichi Kawamoto, Mostafa M. Fouda, and Nei Kato. A Survey on Multi-AP Coordination Approaches Over Emerging WLANs: Future Directions and Open Challenges. *IEEE Communications Surveys & Tutorials*, 26(2):858–889, 2024. ISSN 1553-877X. doi: 10.1109/comst.2023.3344167.

[23] David Nunez, Malcom Smith, and Boris Bellalta. Multi-AP Coordinated Spatial Reuse for Wi-Fi 8: Group Creation and Scheduling. In *21st Mediterranean Communication and Computer Networking Conference (MedComNet 2023)*, pages 203–208, Island of Ponza, Italy, June 2023. IEEE. doi: 10.1109/medcomnet58619.2023.10168857.

[24] M. Seyedebrahimi, F. Bouhafs, A. Raschella, M. Mackay, and Q. Shi. SDN-based channel assignment algorithm for interference management in dense Wi-Fi networks. In *European Conference on Networks and Communications (EuCNC 2016)*, Athens, Greece, June 2016. doi: 10.1109/eucnc.2016.7561018.

[25] Fuad M. Abinader, Sayantan Choudhury, Vicente A. de Sousa, Fabiano S. Chaves, André M. Cavalcante, Erika P. L. Almeida, Robson Vieira, Esa Tuomaala, and Klaus Doppler. Distributed Wi-Fi Interference Coordination for Dense Deployments. *Springer Wireless Personal Communications*, 97(1):1033–1058, June 2017. doi: 10.1007/s11277-017-4550-3.

[26] Shuwei Qiu, Xiaowen Chu, Yiu-Wing Leung, and Joseph Kee-Yin Ng. Joint Access Point Placement and Power-Channel-Resource-Unit Assignment for IEEE 802.11ax-Based Dense WiFi Network With QoS Requirements. *IEEE Transactions on Mobile Computing*, 22(5):2771–2788, May 2023. ISSN 1536-1233. doi: 10.1109/tmc.2021.3129596.

[27] Lorenzo Bertizzolo, Emrecan Demirors, Zhangyu Guan, and Tommaso Melodia. CoBeam: Beamforming-Based Spectrum Sharing With Zero Cross-Technology Signaling for 5G Wireless Networks. In *39th IEEE International Conference on Computer Communications (INFOCOM 2020)*, pages 1429–1438, Virtual Conference, July 2020. IEEE. doi: 10.1109/INFOCOM41043.2020.9155498.

[28] Yang Li, Ting Zhou, Yang Yang, Honglin Hu, and Matti Hamalainen. Fair Downlink Traffic Management for Hybrid LAA-LTE/Wi-Fi Networks. *IEEE Access*, 5:7031–7041, December 2016. ISSN 2169-3536. doi: 10.1109/access.2016.2642121.

[29] Akindele Segun Afolabi, Shehu Ahmed, and Olubunmi Adewale Akinola. A Reinforcement Learning Approach for Interference Management in Heterogeneous Wireless Networks. *International Journal of Interactive Mobile Technologies*, 15(12):65–85, June 2021. ISSN 1865-7923. doi: 10.3991/ijim.v15i12.20751.

[30] Pulok Tarafder and Wooyeol Choi. Deep Reinforcement Learning-Based Coordinated Beamforming for mmWave Massive MIMO Vehicular Networks. *MDPI Sensors*, 23(5):2772, March 2023. ISSN 1424-8220. doi: 10.3390/s23052772.

[31] Ahmed Alkhateeb, Sam Alex, Paul Varkey, Ying Li, Qi Qu, and Djordje Tujkovic. Deep Learning Coordinated Beamforming for Highly-Mobile Millimeter Wave Systems. *IEEE Access*, 6: 37328–37348, June 2018. ISSN 2169-3536. doi: 10.1109/access.2018.2850226.

[32] Jiaxing Wang, Rui Han, Lin Bai, Tao Zhang, Jianwei Liu, and Jinho Choi. Coordinated Beamforming for UAV-Aided Millimeter-Wave Communications Using GPML-Based Channel Estimation. *IEEE Transactions on Cognitive Communications and Networking*, 7(1):100–109, March 2021. ISSN 2332-7731. doi: 10.1109/tccn.2020.3048399.

[33] Changyin Sun, Zhao Shi, and Fan Jiang. A Machine Learning Approach for Beamforming in Ultra Dense Network Considering Selfish and Altruistic Strategy. *IEEE Access*, 8:6304–6315, January 2020. ISSN 2169-3536. doi: 10.1109/access.2019.2963468.

[34] Xiwen Zhang, Tolunay Seyfi, Shengtai Ju, Sharan Ramjee, Aly El Gamal, and Yonina C. Eldar. Deep Learning for Interference Identification: Band, Training SNR, and Sample Selection. In *20th IEEE International Workshop on Signal Processing Advances in Wireless Communications (SPAWC 2019)*, Cannes, France, July 2019. IEEE. doi: 10.1109/spawc.2019.8815481.

[35] Yiming Zhou, Ashkan Samiee, Tingyi Zhou, and Jalal Jalali. Deep Learning Interference Cancellation in Wireless Networks. eess.SP 2009.05533, arXiv, September 2020.

[36] Daniele Croce, Domenico Garlisi, Fabrizio Giuliano, Nicola Inzerillo, and Ilenia Tinnirello. Learning From Errors: Detecting Cross-Technology Interference in WiFi Networks. *IEEE Transactions on Cognitive Communications and Networking*, 2(4): 347–356, December 2016. ISSN 2332-7731. doi: 10.1109/tccn.2018.2816068.

[37] ChunChih Lin, Gen Li, Xiaonan Zhang, and Linke Guo. RF Sensing-enabled Interference Mitigation for Wi-Fi-based IoT Systems: A Deep Learning Approach. In *12th IEEE Conference on Communications and Network Security (CNS 2024)*, pages 1–9, Taipei, Taiwan, September 2024. IEEE. doi: 10.1109/cns62487.2024.10735625.

[38] Garima Mishra, Hemant Kumar Rath, Shameem Nadaf, Raja Mukhopadhyay, and M. Menon. A Reinforcement Learning Approach to Improve WiFi Network Performance Coexisting with LTE. In *13th IEEE International Conference on Communication Systems and Network Technologies (CSNT 2024)*, pages 12–17, Jabalpur, India, April 2024. IEEE. doi: 10.1109/csnt60213.2024.10546221.

[39] Teemu Pulkkinen, Jukka K. Nurminen, and Petteri Nurmi. Understanding WiFi Cross-Technology Interference Detection in the Real World. In *40th IEEE International Conference on Distributed Computing Systems (ICDCS 2020)*, pages 954–964, Singapore, Singapore, November 2020. IEEE. doi: 10.1109/icdcs47774.2020.00061.

[40] Malte Schmidt, Dimitri Block, and Uwe Meier. Wireless interference identification with convolutional neural networks. In *15th IEEE International Conference on Industrial Informatics (INDIN 2017)*, Emden, Germany, July 2017. doi: 10.1109/indin.2017.8104767.

[41] Jinwook Kim, Seongwook Lee, Yong-Hwa Kim, and Seong-Cheol Kim. Classification of Interference Signal for Automotive Radar Systems With Convolutional Neural Network. *IEEE Access*, 8: 176717–176727, January 2020. ISSN 2169-3536. doi: 10.1109/access.2020.3026749.

[42] Clifton Paul Robinson, Daniel Uvaydov, Salvatore D'Oro, and Tommaso Melodia. Narrowband Interference Detection via Deep Learning. In *IEEE International Conference on Communications (ICC 2023)*, pages 6379–6384, Rome, Italy, May 2023. IEEE. doi: 10.1109/icc45041.2023.10278618.

[43] Andreas Andersson, Patrik Eliardsson, Erik Axell, Kristoffer Hägglund, and Kia Wiklundh. Deep Learning-Based In-Band Interference Detection and Classification. *IEEE Transactions on Electromagnetic Compatibility*, pages 1–9, September 2024. ISSN 1558-187X. doi: 10.1109/temc.2024.3449434.

[44] Ayesha Hasan and Bilal Muhammad Khan. Deep learning aided wireless interference identification for coexistence management in the ISM bands. *Wireless Networks*, 29(7):3311–3331, June 2023. ISSN 1572-8196. doi: 10.1007/s11276-023-03389-3.

[45] Hyung Jun Kwon, Jung Hoon Lee, and Wan Choi. Machine Learning-Based Beamforming in K-User MISO Interference Channels. *IEEE Access*, 9:28066–28075, February 2021. ISSN 2169-3536. doi: 10.1109/access.2021.3058759.

[46] Hao Huang, Wenchao Xia, Jian Xiong, Jie Yang, Gan Zheng, and Xiaomei Zhu. Unsupervised Learning-Based Fast Beamforming Design for Downlink MIMO. *IEEE Access*, 7:7599–7605, December 2018. ISSN 2169-3536. doi: 10.1109/access.2018.2887308.

[47] Lyutianyang Zhang, Hao Yin, Sumit Roy, and Liu Cao. Multiaccess Point Coordination for Next-Gen Wi-Fi Networks Aided by Deep Reinforcement Learning. *IEEE Systems Journal*, 17(1): 904–915, March 2023. ISSN 1932-8184. doi: 10.1109/jsyst.2022.3183199.

[48] Yuto Kihira, Yusuke Koda, Koji Yamamoto, Takayuki Nishio, and Masahiro Morikura. Adversarial Reinforcement Learning-based Robust Access Point Coordination Against Uncoordinated Interference. In *92nd IEEE Vehicular Technology Conference (VTC 2020-Fall)*, pages 1–5, Virtual Conference, November 2020. IEEE. doi: 10.1109/vtc2020-fall49728.2020.9348462.

[49] Arpan Pal, Amit Mehta, Andrew Skippins, Paul Spicer, and Dariush Mirshekar-Syahkal. Novel Interference Suppression Null Steering Antenna System for High Precision Positioning. *IEEE Access*, 8:77779–77787, 2020. ISSN 2169-3536. doi: 10.1109/access.2020.2988881.

[50] Shivam Chauhan, Arpit Sharma, Shivam Pandey, Kowtharapu Nageswara Rao, and Pradeep Kumar. IEEE 802.11be: A Review on Wi-Fi 7 Use Cases. In *9th International Conference on Reliability, Infocom Technologies and Optimization (ICRITO 2021)*, Noida, India, September 2021. IEEE. doi: 10.1109/icrito51393.2021.9596344.

[51] Ehab Mahmoud Mohamed, Hideyuki Kusano, Kei Sakaguchi, and Seiichi Sampei. WiFi assisted multi-WiGig AP coordination for future multi-Gbps WLANs. In *IEEE Pacific Rim Conference on Communications, Computers and Signal Processing (PACRIM 2001)*, Victoria, Canada, August 2001. IEEE. ISBN 978-0-7803-7080-7. doi: 10.1109/pimrc.2015.7343623.

[52] Ehab Mahmoud Mohamed, Kei Sakaguchi, and Seiichi Sampei. Wi-Fi Coordinated WiGig Concurrent Transmissions in Random Access Scenarios. *IEEE Transactions on Vehicular Technology*, 66(11):10357–10371, November 2017. ISSN 1939-9359. doi: 10.1109/tvt.2017.2738198.

[53] Ding Zhang, Panneer Selvam Santhalingam, Parth Pathak, and Zizhan Zheng. CoBF: Coordinated Beamforming in Dense mmWave Networks. *Proceedings of the ACM on Measurement and Analysis of Computing Systems*, 7(2):1–26, June 2023. ISSN 2476-1249. doi: 10.1145/3589975.

[54] Cailian Deng, Xuming Fang, Xiao Han, Xianbin Wang, Li Yan, Rong He, Yan Long, and Yuchen Yan Long. IEEE 802.11be Wi-Fi 7: New Challenges and Opportunities. *IEEE Communications Surveys & Tutorials*, 22(4):2136–2166, 2020. ISSN 1553-877X. doi: 10.1109/comst.2020.3012715.

[55] Hayssam Dahrouj and Wei Yu. Coordinated beamforming for the multicell multi-antenna wireless system. *IEEE Transactions on Wireless Communications*, 9(5):1748–1759, May 2010. ISSN 1536-1276. doi: 10.1109/twc.2010.05.090936.

[56] Amin Azari and Meysam Masoudi. Interference management for coexisting Internet of Things networks over unlicensed spectrum. *Elsevier Ad Hoc Networks*, 120:102539, September 2021. ISSN 1570-8705. doi: 10.1016/j.adhoc.2021.102539.

[57] Mingzhe Chen, Walid Saad, and Changchuan Yin. Virtual Reality Over Wireless Networks: Quality-of-Service Model and Learning-Based Resource Management. *IEEE Transactions on Communications*, 66(11):5621–5635, November 2018. ISSN 1558-0857. doi: 10.1109/tcomm.2018.2850303.

[58] Hazimf Shakhatreh, Ahmad Sawalmeh, Khaled F. Hayajneh, Sharief Abdel-Razeq, Wa'Ed Malkawi, and Ala Al-Fuqaha. A Systematic Review of Interference Mitigation Techniques in Current and Future UAV-Assisted Wireless Networks. *IEEE Open Journal of the Communications Society*, 5:2815–2846, 2024. ISSN 2644-125X. doi: 10.1109/ojcoms.2024.3392623.

[59] Lorenzo Galati-Giordano, Giovanni Geraci, Marc Carrascosa, and Boris Bellalta. What will Wi-Fi 8 Be? A Primer on IEEE 802.11bn Ultra High Reliability. *IEEE Communications Magazine*, 62(8):126–132, August 2024. ISSN 0163-6804. doi: 10.1109/mcom.001.2300728.

[60] Han Li, Tiejun Lv, and Xuewei Zhang. Deep Deterministic Policy Gradient Based Dynamic Power Control for Self-Powered Ultra-Dense Networks. In *IEEE Global Communications Conference (GLOBECOM 2018), Workshops*, pages 1–6, Abu Dhabi, United Arab Emirates, December 2018. IEEE. ISBN 978-1-5386-4920-6. doi: 10.1109/glocomw.2018.8644157.

[61] Arslan Qadeer and Myung Jong Lee. Deep-Deterministic Policy Gradient Based Multi-Resource Allocation in Edge-Cloud System: A Distributed Approach. *IEEE Access*, 11:20381–20398, 2023. ISSN 2169-3536. doi: 10.1109/access.2023.3249153.

[62] Ebrahim Hamid Sumiea, Said Jadid Abdulkadir, Hitham Seddig Alhussian, Safwan Mahmood Al-Selwi, Alawi Alqushaibi, Mohammed Gamal Ragab, and Suliman Mohamed Fati. Deep deterministic policy gradient algorithm: A systematic review. *Heliyon*, 10(9):30697, May 2024. ISSN 2405-8440. doi: 10.1016/j.heliyon.2024.e30697.

[63] Mohammad Dehghani Soltani, Ardimas Andi Purwita, Zhihong Zeng, Cheng Chen, Harald Haas, and Majid Safari. An Orientation-Based Random Waypoint Model for User Mobility in Wireless Networks. In *IEEE International Conference on Communications (ICC 2020), Workshops*, Virtual Conference, June 2020. IEEE. ISBN 978-1-7281-7440-2. doi: 10.1109/iccworkshops49005.2020.9145333.

[64] G. J. Bastien, P. A. Willems, B. Schepens, and N. C. Heglund. Effect of load and speed on the energetic cost of human walking. *European Journal of Applied Physiology*, 94(1–2):76–83, January 2005. ISSN 1439-6327. doi: 10.1007/s00421-004-1286-z.

[65] Heejung Yu and Taejoon Kim. Beamforming Transmission in IEEE 802.11ac under Time-Varying Channels. *Hindawi The Scientific World Journal*, 2014, 2014. ISSN 1537-744X. doi: 10.1155/2014/920937.

[66] F. Juan Carlos Vesga, H. Martha Fabiola Contreras, and B. Jose Antonio Vesga. Design of empirical propagation models supported in the Log-Normal Shadowing model for the 2.4GHz and 5GHz bands under Indoor environments. *Indian Journal of Science and Technology*, 11(22):1–18, June 2018. ISSN 0974-6846. doi: 10.17485/ijst/2018/v11i22/122149.

[67] Dong Zhou and Ten-Hwang Lai. A Compatible and Scalable Clock Synchronization Protocol in IEEE 802.11 Ad Hoc Networks. In *International Conference on Parallel Processing (ICPP 2005)*, pages 295–302, Oslo, Norway, June 2005. IEEE. doi: 10.1109/icpp.2005.6.

[68] Timothy P. Lillicrap, Jonathan J. Hunt, Alexander Pritzel, Nicolas Heess, Tom Erez, Yuval Tassa, David Silver, and Daan Wierstra. Continuous control with deep reinforcement learning. cs.LG 1509.02971, arXiv, September 2015.

[69] Diederik P. Kingma and Jimmy Ba. Adam: A Method for Stochastic Optimization. cs.LG 1412.6980, arXiv, December 2014.

[70] Megh Bhatt, Ronak Chokshi, Swapneel Desai, Sooksan Panichpapiboon, Nawaporn Wisitpongphan, and Ozan K. Tonguz. Impact of Mobility on the Performance of Ad Hoc Wireless Networks. In *58th IEEE Vehicular Technology Conference (VTC 2003-Fall)*, volume 5, pages 3025–3029, Orlando, FL, October 2003. IEEE.